Low Lithium Concentration Effects on Tracer Diffusion in Amorphous LixSi

Prof. John Taylor[1], Dr. Richard Green[2] & Dr. Sarah Williams[*3]

[1]Department of Neuroscience, University of Oxford, Oxford, UK

[2]Department of Physiology, University of Cambridge, Cambridge, UK

[3]Department of Medical Research, Imperial College London, London, UK

Abstract Li tracer self-diffusion was studied in amorphous lithium-silicon compounds which are important as negative electrodes in Li-ion batteries. Experiments were done on $Li_xSi/^6Li_xSi$ (Li_xSi, $x \sim 0.02$ and $x \sim 0.06$) thin-film hetero-structures using secondary ion mass spectrometry. The diffusivities follow the Arrhenius law in the temperature range between 140 and 325 °C both with an activation energy of (1.42 ± 0.03) eV, while the Li-richer samples show one order of magnitude higher diffusivities. A trap-limited diffusion mechanism is suggested, explaining this result with a lower concentration of unsaturated traps. A discussion against literature suggests a strong lithium concentration dependence of diffusivities also for higher x.

1. Introduction

The scope of sustainable use of resources and slowing down the release of greenhouse gases requires progress in efficient energy storage in rechargeable batteries. Here, Li-ion batteries (LIB) are considered as the system of choice.[1–8] The main advantages of this battery system against conventional systems are the low weight and high energy density available.[3] For future demands improvements in cycle life, safety aspects, costs and especially specific electrode capacity (charge to be stored) connected with increased energy density/power density are required.

A promising high capacity negative electrode material for future applications is amorphous silicon (a-Si) with its enormous theoretical specific capacity of about 4000 mAh/g.[9–16] During electrochemical lithiation at room temperature, lithium forms an amorphous alloy according to the reaction $Si + x\ Li^+ + x\ e^- \leftrightarrow Li_xSi$ ($x \sim 4$). As of late, there are attempts to use not pure Si as active material in the electrode but Li_xSi compounds.[17–21] The aim is to reduce initial capacity losses due to formation of a Solid Electrolyte Interphase or irreversible Li trapping[17,20] and a better contact to the current collector (electrical conductivity). Also a tunable specific capacity could be realized.[18]

Concerning lithiation and delithiation of Si and Li_xSi electrodes, kinetic processes in the interior of the electrode and at surfaces play an important role for a fundamental understanding. There, the Li diffusion in Si and Li_xSi determines charging/discharging times, maximum capacity, self-discharge, power density, and cycling stability. In this context, an important question is also whether electrode lithiation is a lithium diffusion- or interface-reaction-controlled process. Consequently, a reliable experimental determination of atomic/ionic transport properties is highly desirable.

In literature, the experimental determination of chemical diffusivities in silicon electrodes is nearly exclusively carried out by electrochemical methods like cyclic voltammetry (CV),[22–25] electrochemical impedance spectroscopy (EIS)[26,27] and potentiostatic or galvanostatic intermittent titration technique (PITT/GITT)[26–28]. These diffusivities vary in a relatively unsystematic way between 10^{-14} and 10^{-18} m^2/s close to room temperature and are heavily based on appropriate model assumptions which are not always fulfilled. Consequently, the aim of the present paper is the determination of Li tracer self-diffusivities independently using stable tracer methods. Here, we present the first Li tracer diffusion measurements in an amorphous lithium-silicon compound a-Li_xSi. Experiments were done on Li_xSi/^6Li_xSi hetero-structures using secondary ion mass spectrometry (SIMS). As model system we chose a-Li_xSi with a relatively low Li content, which is especially important for the initial lithiation stages.

2. Experimental Methods

For the presented experiments, amorphous [$^{nat}Li_xSi$ (90 nm) | ^6Li_xSi (90 nm)] structures were produced by ion-beam co-sputter deposition in an ion-beam sputtering unit (IBC 681, Gatan) onto commercial (100) oriented silicon wafers. Argon (purity: 99.996 %) was used as sputter gas. Specially designed, segmented targets were used where parts of lithium metal and of a nominally undoped silicon wafer (prime, MicroChemicals GmbH, Germany) were fixed on a steel support (surface ratio Li:Si = 1:4 or 1:3 respectively) completely covering the steel surface. The general technique has been outlined in a previous publication.[29] The design chosen in this study led to a relative lithium fraction of $x \sim 0.02$ or $x \sim 0.06$ in the two different types of Li_xSi layers produced. The lithium fraction was determined by X-ray photoelectron spectroscopy using a K-Alpha XPS spectrometer (ThermoFisher Scientific, East Grinstead, UK) after removing several tens of nanometers from the sample by Ar ion sputtering. These values are a relatively rough estimate due to the extremely low photoionization cross-section of Li.[30] $^{nat}Li_xSi$ was deposited using lithium foil (99.9 % purity, Alfa Aesar, Germany) and nominally undoped

silicon wafer material while the $^{6}Li_xSi$ layers necessitated ^{6}Li lumps molded into the required shape. Structural investigation was done by grazing-incidence X-ray diffractometry measurements of sputtered films in the as-deposited state and after annealing for 20 h at 300 °C, close to the highest temperature under investigation. All samples are X-ray amorphous. Annealing was performed in an AO500 rapid thermal annealing setup (MBE components) in argon atmosphere. Depth profiles of isotope fractions were obtained by SIMS using a Cameca ims3f/4f with O_2^+ primary ions. Analysis of the resulting sputter craters was performed by stylus profilometry using a Tencor Alphastep 500.

3. Results

Fig. 1 shows a comparison of the relative ^{7}Li isotope fraction, *c*, for the as-deposited sample (fig. 1a) and the same sample annealed at 250 °C for 4 min (fig. 1b). The isotope fraction is calculated from the ^{6}Li and ^{7}Li signal intensities *I* as measured by SIMS as

$$c = \frac{I\left(^{7}\mathrm{Li}\right)}{I\left(^{6}\mathrm{Li}\right) + I\left(^{7}\mathrm{Li}\right)}. \tag{1}$$

Both curves are plotted against the sputter depth. For better visibility of the interface broadening only the region where the isotope content is subject to rapid change is shown.

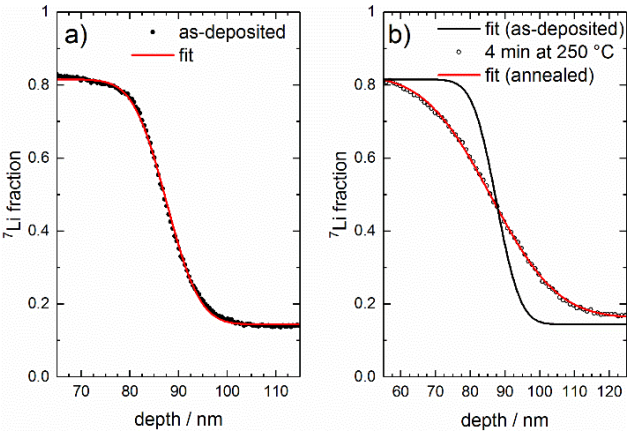

Figure 1:

Depth profiles of $^{nat}Li_xSi/^{6}Li_xSi$ double layer structures (x ~ 0.02) as obtained by SIMS. The ^{7}Li isotope fraction is shown as a function of sputter depth. The depiction is limited to the interface region to better assess the broadening. a) as-deposited state and b) comparison of as-deposited and annealed state (4 min at 250 °C). Also shown are fits according to eq. (2).

Lithium diffusion is reflected in a broadening of the measured curve of the annealed sample in this interface region when compared to the as-deposited state. This effect is clearly visible in the comparative depiction in fig. 1b. Diffusivities can be determined by using the following solution to Fick's second law pertaining to diffusion across an interface[31]

$$c(x,t) = c_\infty + \frac{(c_0 - c_\infty)}{2}\left[\operatorname{erf}\left(\frac{h+x}{R}\right) + \operatorname{erf}\left(\frac{h-x}{R}\right)\right]. \quad (2)$$

Here, c_∞ is the residual ^{7}Li concentration in the layer adjacent to the substrate, c_0 the ^{7}Li concentration present in the top layer, h the thickness of the $^{nat}Li_xSi$ layer as determined by SIMS measurements in the as-deposited state and R is the broadening of the curve at the interface. In fig. 1a a least squares fit according to equation (2) with R treated as a fit parameter is shown together with the measured data. The initial broadening of the as-deposited state of the sample shown in fig. 1a is determined as $R(0) = (7.7 \pm 0.1)$ nm. After annealing the sample for 4 min at 250 °C the broadening increases to $R(t) = (19.8 \pm 0.2)$ nm, as can be derived from the fit to the data shown in fig. 1b. Diffusivities D after annealing for a time t can then be calculated from the change in broadening compared to the as-deposited state according to $D(t) = \left(R^2(t) - R^2(0)\right)/4t$. The diffusivity at 250 °C is determined to (3.5 ± 1.7) × 10^{-19} m²/s.

In order to investigate a possible dependence of the diffusivities on annealing time, a single sample of the same composition was annealed successively for increasing time periods at 200 °C. Fig 2a shows the resulting ^{7}Li depth profiles obtained for the as-deposited state as well as after annealing at 200 °C for 15, 60 and 240 min, respectively. Again, the broadening R was obtained by fitting equation (2) to the data. The resulting diffusivities for all three annealing

steps are plotted in fig. 2b against the annealing time. All calculated values are in the order of $D = 1\times10^{-20}$ m²/s and identical within error limits. This result excludes a significant time dependence of the diffusivities in the investigated time-range.

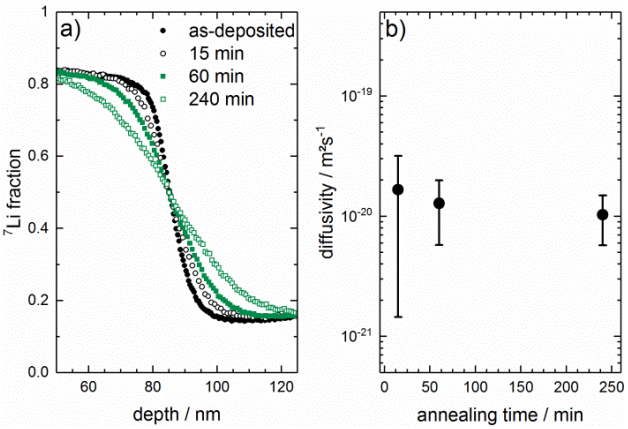

Figure 2:

a) ^{7}Li isotope fraction depth profiles as obtained from SIMS of $^{nat}Li_xSi/^6Li_xSi$ double layer structures (x ~ 0.02) successively annealed at 200 °C for increasing duration up to 240 min. b) Corresponding calculated diffusivities plotted against the annealing time.

Fig. 3 depicts all diffusivities derived from the SIMS measurements plotted against the reciprocal temperature, T, for the two types of samples under investigation. For the sample with x ~ 0.02 diffusivities span five orders of magnitude from 10^{-17} to 10^{-22} m²/s between 140 and 325 °C. The diffusivities obey the Arrhenius law

$$D = D_0 \exp\left(\frac{-E_a}{k_B T}\right) \tag{3}$$

with the activation energy E_a and the pre-exponential factor D_0 while k_B is the Boltzmann constant. The activation energy found for the presented data is $E_a = (1.42 \pm 0.03)$ eV and the pre-exponential factor is $D_0 = 1.8\times10^{-5}$ m²/s (error: $\log_{10}\left(D_0 / \mathrm{m^2 s^{-1}}\right) = 0.3$). The second dataset with a higher Li content of x ~ 0.06 shows diffusivities that are higher by about one order of magnitude. These diffusivities can also be described by eq. (3) with the same activation

energy and a pre-exponential factor of $D_0 = 1.5\times10^{-4}$ m²/s. A free fit of the data yields an activation energy of $E_a = (1.38 \pm 0.07)$ eV which is identical within error limits.

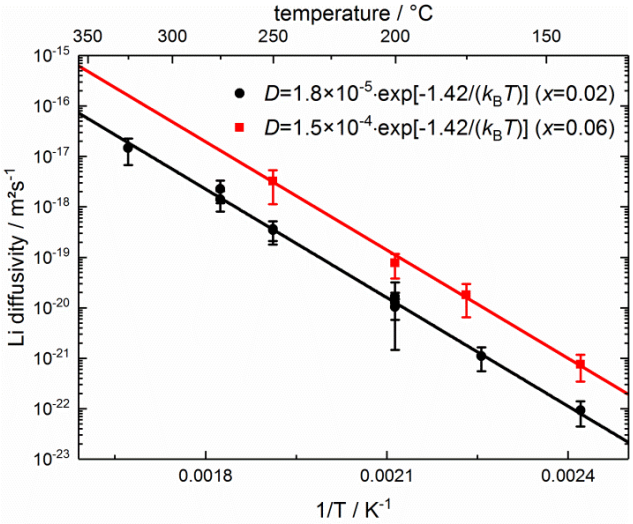

Figure 3: Li diffusivities *D* plotted against the reciprocal temperature. The straight lines represent fits of the Arrhenius law (eq. (3)) to the diffusivities.

4. Discussion

The presented data allows the conclusion that an increase in Li content from x ~ 0.02 to x ~ 0.06 leads to a faster Li diffusion in amorphous Li_xSi. Available literature data support this conclusion, albeit not for Li contents as low as in the present samples. The most likely explanation for the acceleration of diffusion found in this study is a change in the concentration of trapping sites in the material assuming a trap-limited diffusion mechanism. Both aspects are discussed in the following paragraphs.

In fig. 4 the diffusivities obtained in this study are compared to literature data on similar types of materials. The relatively low Li fraction of the samples investigated suggests a direct comparison to Li diffusivities in amorphous and also crystalline silicon. Li diffusivities in crystalline silicon (c-Si) have been reported as early as 1960 by Pell[32] (*a* in fig. 4) and some years later by Larue[33] (*b* in fig. 4). Both publications examine different temperature ranges but

agree in their findings in the respective extrapolated data. Both report activation energies in the range of about 0.7 eV. This is assigned to a diffusion mechanism along interstitial sites in the c-Si structure, which is considerably faster than found in this study.

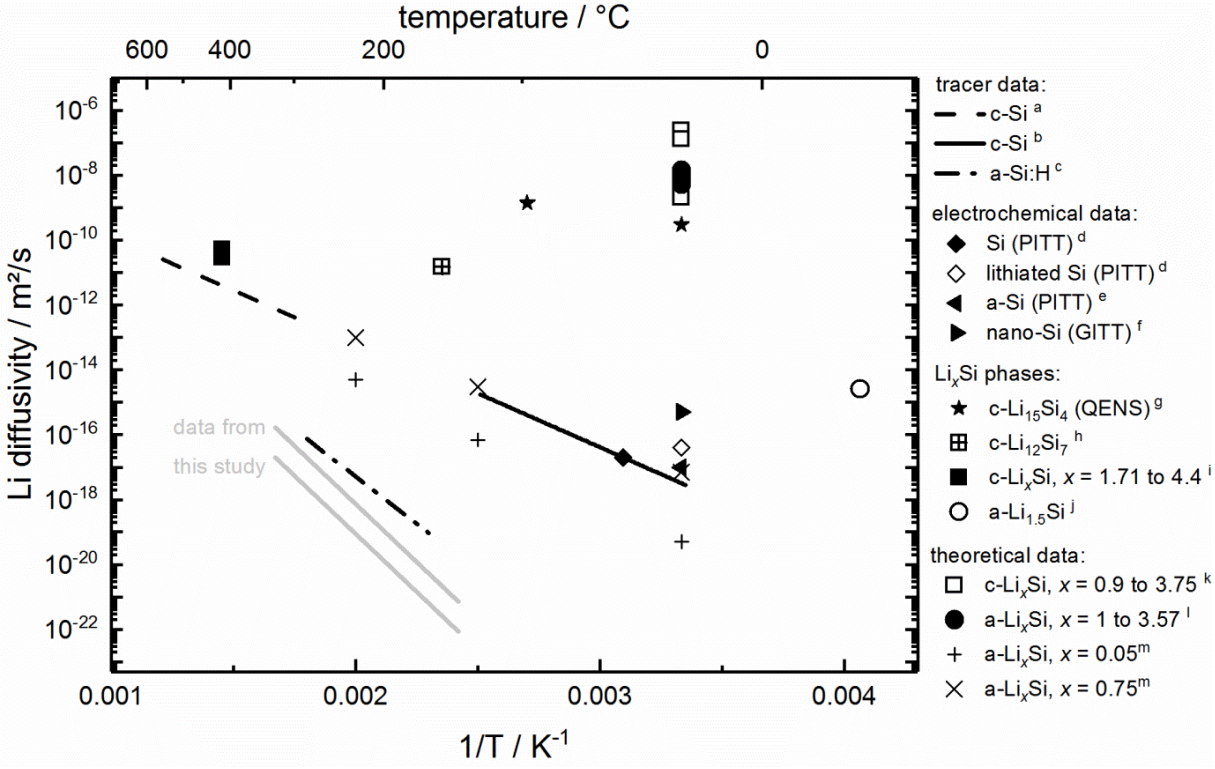

Figure 4:

Li diffusivities as given in literature plotted against the reciprocal temperature in comparison to the experimental data of this study. Data are split into four groups: tracer diffusivity measurements on silicon (a[33], b[32], and c[34]), data acquired by electrochemical methods (d[26], e[28] and f[27]), diffusivities of Li_xSi phases (g[35], h[36], i[37] and j[38]) and theoretical calculations of Li diffusivities in Li_xSi with varying values for x (k[39], l[40] and m[41]). In this context "c-" denotes crystalline and "a-" amorphous.

Li diffusion studies in hydrogenated a-Si were done by Zastrow et al. (*c* in fig. 4) in a similar temperature range as chosen in the present study. Their results are very close to our results on Li_xSi ($x \sim 0.06$) and show a similar activation energy of $E_a = 1.15$ eV.[34] Furthermore, they give a pre-exponential factor of 2×10^{-6} m²/s, deviating only by one order of magnitude from the value derived from the fit to the low Li content data ($x \sim 0.02$) in fig. 3. Consequently, the principal mechanism of diffusion seems to be at least comparable.

In the a-Si modification there is no clearly defined interstitial pathway. In addition to that, a-Si exhibits a rather high concentration of intrinsic defects formed by threefold coordinated silicon atoms, so called dangling bonds (DB).[42,43] Concurrently, the data reported on Li diffusion in a-Si exhibit lower absolute diffusivities and differing activation energies when compared with data for c-Si. Beyer and Zastrow suggested a trap-limited diffusion mechanism to explain their results.[44] Basically, trap-limited diffusion describes an interstitial mobility of atoms that is correlated with the formation of complexes at trapping centers. In an a-Si network traps are most likely DBs where Li will be trapped with a certain probability but can also be thermally dissociated from these centers again.[45]

From the findings reported here, a trap-limited mechanism seems to be also governing diffusion in a-Li_xSi with low values of x as studied here. The activation energy of diffusion is then given by the sum of the migration energy of free Li, E_m, and the binding energy of Li to the trap, E_b. The latter quantity can be estimated to $E_b \approx 0.7$ eV if $E_m \approx 0.7$ eV (interstitial Li diffusion in c-Si) is assumed.[32,33] The bond energy of Li to the trap of 0.7 eV is relatively low compared to the Li-Si bond dissociation energy of a diatomic molecule of 1.55 eV as given in literature.[46] Consequently we can speak of a shallow trap.[47]

Furthermore, the trap-limited diffusion model can be applied to analyze the pre-exponential factor in more detail. For a closer look at the pre-exponential factor, a model previously used e.g. for hydrogen diffusion in a-Si:H can be employed to assess trap concentrations.[49] The trap concentration T_0 can be calculated from the pre-exponential factor D_0 according to $T_0 = \nu_0 / (4\pi R_c D_0)$ with the attempt frequency $\nu_0 = 1.3\times10^{13}\ s^{-1}$, which is in most cases identical to the Debye frequency of the material (here the value for a-Si was chosen),[50] and the effective trap radius $R_c \approx 5\times10^{-10}$ m.[51] For the sample with lower Li content (x ~ 0.02) a trap concentration of $T_0 = 1.2\times10^{20}\ cm^{-3}$ is found. This compares well with literature data on trap

density for a-Si:H prepared by a glow-discharge technique and makes the assumption of a trap-limited diffusion plausible.[47] For the sample with higher Li concentration we can derive from the higher pre-exponential factor a lower trap concentration of $T_0 = 1.2 \times 10^{19}$ cm^{-3}. Thus faster diffusion is realized by a lower amount of traps in the sample. This can be explained with the fact that DBs (or other intrinsic defects) present in the a-Li$_x$Si layers after deposition might be saturated by Li atoms, at least partly. The higher Li concentration has the consequence that the number of unsaturated traps is reduced and diffusion is accelerated. This might also explain the findings by Zastrow et al..[34] In their study, hydrogen is used to saturate DBs in the material. Those trapping sites are then not readily available for Li atoms. In literature there are no experimental studies that directly compare Si and Li$_x$Si samples (especially with low *x*) produced in an identical way (preferably in the same laboratory). Consequently, conclusions drawn from a comparison of hydrogenated and lithiated a-Si have to be handled with care.

In theoretical work the trapping site theory is most notably supported by the finding of Tritsaris et al..[48] They find a distribution of activation energies for diffusive motion in bulk a-Si but discuss several distinct processes. One of those is a jump to a trapping site where the reverse jump from the site needs an activation energy of 1.46 eV, a value identical to that presented in our study.

In literature there are also experimental studies on Li diffusion in Li$_x$Si materials with high values of *x*. Independent from the crystallinity of the samples (or lack thereof) reported diffusivities for Li$_x$Si with high *x* are always faster than those found for c-Si by Pell and Larue[32,33] and for our results with low *x*. Dunst et al. give a diffusivity of 2.6×10^{-15} m²/s for electrochemically amorphized Li$_{1.5}$Si, determined by NMR spectroscopy at -30 °C (*j* in fig. 4).[38] Also determined by NMR are results by Kuhn et al. on (crystalline) Li$_{12}$Si$_7$ (*h* in fig. 4).[36] They find a diffusion coefficient of 10^{-11} m²/s at 150 °C. A further study by Sacci et al. with quasi-elastic neutron scattering (QENS) on Li$_{15}$Si$_4$ yields diffusivities in the order of 10^{-10} m²/s and

an assessed very low activation energy of only 0.2 eV (*g* in fig. 4).[35] They propose that the less Li is bonded with Si, the more it is able to move freely and thus with low activation energies (interstitial-like diffusion). Wen et al. provide data for Li diffusion in various crystalline Li_xSi phases at 400 °C obtained from coulometric titration (*i* in fig. 4), surpassing the diffusivities given for c-Si by at least one order of magnitude.[37]

Additional data in literature were obtained using electrochemical methods such as galvanostatic or potentiostatic intermittent titration technique (GITT/PITT) during the lithiation of silicon. In that case chemical diffusivities for Li_xSi materials with high values of *x* are probed (*d*, *e*, *f* in fig. 4).[26–28] All values obtained by those methods are much higher than those found when our diffusivities are extrapolated to room temperature. As already pointed out earlier, these data rely heavily on specific model assumptions and thus are prone to certain variations. A direct comparison is problematic since our experiments determine tracer diffusivities while electrochemical methods measure chemical diffusivities. In addition, the “synthesis route” of the material (electrochemically, sputter deposition) can produce essentially different results.

Concerning theoretical calculations, two studies should be addressed: For amorphous (*l* in fig. 4)[40] and crystalline Li_xSi (*k* in fig. 4)[39] (for $x \geq 1$) an increase in Li diffusivities of up to two orders of magnitude is found when *x* is raised. Theoretical calculations were also done by Fedorov et al. spanning values for *x* from 0.05 to 0.75 (*m* in fig. 4).[41] They clearly show an increase in diffusivities over roughly two orders of magnitude with increasing *x*. They also compare the data to similar calculations for crystalline Li_xSi with the same Li concentrations. However, their findings that Li diffusivity in the crystalline modifications is about one order of magnitude slower than in the same amorphous phase is contradicted by our data and those of Zastrow. In addition to that, their absolute values for diffusivities in the amorphous phase are up to six orders of magnitude faster than found in our experiments.

From this literature discussion two important results can be derived. First, samples with a high *x* in Li_xSi show considerable faster diffusion than those with low *x*. Further, samples with a low value of *x* do not necessarily show faster diffusion than pure Si. Everything depends on the details of the trap-limited diffusion process.

5. Conclusions and Outlook

In conclusion, lithium tracer self-diffusion in amorphous [$^{nat}Li_xSi$ (90 nm) | $^{6}Li_xSi$ (90 nm)] (x ~ 0.02 and 0.06) structures was investigated using secondary ion mass spectrometry. For samples with x ~ 0.02 diffusivities spanning five orders of magnitude from 10^{-17} to 10^{-22} m^2/s were determined by comparing the broadening of ^{7}Li depth profiles prior to and after annealing steps at temperatures between 140 and 325 °C. The diffusivities follow the Arrhenius law yielding an activation energy of (1.42 ± 0.03) eV. Increasing the Li content of the samples to *x* ~ 0.06 results in a diffusion that is overall faster by one order of magnitude but is still described by the same activation energy. This can be explained within the framework of the trap-limited diffusion theory and a lower concentration of unsaturated traps. A time-dependence of diffusivities could be ruled out. The Li diffusion is several orders of magnitude lower than in crystalline Si where Li diffuses via an interstitial mechanism. Comparison to literature data on Li_xSi samples with high *x* as well as to theoretical calculations suggests a much faster diffusion of Li for high values of *x*, while showing considerable scatter over several orders of magnitude. Consequently, there is a strong need for detailed diffusion studies as a function of Li concentration in Li_xSi done by the same method and samples all prepared in the same way. Only from these results a clear picture of the influence of Li concentration on diffusion can be drawn.

References

(1) *High energy density lithium batteries: Materials, engineering, applications;* Aifantis, K. E., Ed.; Wiley-VCH-Verl.: Weinheim, 2010.

(2) Goodenough, J. B.; Park, K.-S. The Li-ion rechargeable battery: A perspective. *J. Am. Chem. Soc.* **2013**, *135*, 1167–1176.

(3) Bruce, P. G.; Scrosati, B.; Tarascon, J.-M. Nanomaterials for rechargeable lithium batteries. *Angewandte Chemie (International ed. in English)* **2008**, *47*, 2930–2946.

(4) Etacheri, V.; Marom, R.; Elazari, R.; Salitra, G.; Aurbach, D. Challenges in the development of advanced Li-ion batteries: A review. *Energy Environ. Sci.* **2011**, *4*, 3243–3262.

(5) Chen, J.; Cheng, F. Combination of lightweight elements and nanostructured materials for batteries. *Accounts of chemical research* **2009**, *42*, 713–723.

(6) Lu, L.; Han, X.; Li, J.; Hua, J.; Ouyang, M. A review on the key issues for lithium-ion battery management in electric vehicles. *Journal of Power Sources* **2013**, *226*, 272–288.

(7) Manthiram, A.; Murugan, A. V.; Sarkar, A.; Muraliganth, T. Nanostructured electrode materials for electrochemical energy storage and conversion. *Energy Environ. Sci.* **2008**, *1*, 621–638.

(8) Patil, A.; Patil, V.; Wook Shin, D.; Choi, J.-W.; Paik, D.-S.; Yoon, S.-J. Issue and challenges facing rechargeable thin film lithium batteries. *Materials Research Bulletin* **2008**, *43*, 1913–1942.

(9) McDowell, M. T.; Lee, S. W.; Nix, W. D.; Cui, Y. 25th anniversary article: Understanding the lithiation of silicon and other alloying anodes for lithium-ion batteries. *Adv. Mater. Weinheim* **2013**, *25*, 4966–4985.

(10) Wang, C.; Wu, H.; Chen, Z.; McDowell, M. T.; Cui, Y.; Bao, Z. Self-healing chemistry enables the stable operation of silicon microparticle anodes for high-energy lithium-ion batteries. *Nature chemistry* **2013**, *5*, 1042–1048.

(11) Bourderau, S.; Brousse, T.; Schleich, D.M. Amorphous silicon as a possible anode material for Li-ion batteries. *Journal of Power Sources* **1999**, *81-82*, 233–236.

(12) Jung, H.; Park, M.; Han, S. H.; Lim, H.; Joo, S.-K. Amorphous silicon thin-film negative electrode prepared by low pressure chemical vapor deposition for lithium-ion batteries. *Solid State Communications* **2003**, *125*, 387–390.

(13) Ohara, S.; Suzuki, J.; Sekine, K.; Takamura, T. A thin film silicon anode for Li-ion batteries having a very large specific capacity and long cycle life. *Journal of Power Sources* **2004**, *136*, 303–306.

(14) Moon, T.; Kim, C.; Park, B. Electrochemical performance of amorphous-silicon thin films for lithium rechargeable batteries. *Journal of Power Sources* **2006**, *155*, 391–394.

(15) Baranchugov, V.; Markevich, E.; Pollak, E.; Salitra, G.; Aurbach, D. Amorphous silicon thin films as a high capacity anodes for Li-ion batteries in ionic liquid electrolytes. *Electrochemistry Communications* **2007**, *9*, 796–800.

(16) Beattie, S. D.; Loveridge, M. J.; Lain, M. J.; Ferrari, S.; Polzin, B. J.; Bhagat, R.; Dashwood, R. Understanding capacity fade in silicon based electrodes for lithium-ion batteries using three electrode cells and upper cut-off voltage studies. *Journal of Power Sources* **2016**, *302*, 426–430.

(17) Zhao, J.; Lu, Z.; Liu, N.; Lee, H.-W.; McDowell, M. T.; Cui, Y. Dry-air-stable lithium silicide-lithium oxide core-shell nanoparticles as high-capacity prelithiation reagents. *Nature communications* **2014**, *5*, 5088.

(18) Lü Rong-Guan, Yang Jun, Wang Jiu-Lin, Nuli Yan-Na. Electrodeposition and Electrochemical Property of Porous Li-Si Film Anodes for Lithium-Ion Batteries. *Acta Physico-Chimica Sinica* **2011**, *27*, 759.

(19) Zhamu, A.; Shi, J.; Chen, G.; Fang, Q.; Jang, Bor Z.Aruna Zhamu, Jinjun Shi, Guorong Chen, Qing Fang, Bor Z. Jang. Graphene-enhanced anode particulates for lithium ion batteries. US 12/807,635, Sep 10, 2010.
(20) Wu, J. Study of Prelithiated Silicon As Anode in Lithium-Ion Cells. *Meet. Abstr.* **2014**, *MA2014-01*, 196.
(21) Cloud, J. E.; Wang, Y.; Li, X.; Yoder, T. S.; Yang, Y.; Yang, Y. Lithium silicide nanocrystals: Synthesis, chemical stability, thermal stability, and carbon encapsulation. *Inorganic chemistry* **2014**, *53*, 11289–11297.
(22) Xiao, X.; Liu, P.; Verbrugge, M. W.; Haftbaradaran, H.; Gao, H. Improved cycling stability of silicon thin film electrodes through patterning for high energy density lithium batteries. *Journal of Power Sources* **2011**, *196*, 1409–1416.
(23) Kulova, T. L.; Skundin, A. M.; Pleskov, Y.V.; Terukov, E. I.; Kon'kov, O. I. Lithium insertion into amorphous silicon thin-film electrodes. *Journal of Electroanalytical Chemistry* **2007**, *600*, 217–225.
(24) Arie, A. A.; Lee, J. K. A study of Li-ion diffusion kinetics in the fullerene-coated Si anodes of lithium ion batteries. *Phys. Scr.* **2010**, *2010*, 14013.
(25) Yoshimura, K.; Suzuki, J.; Sekine, K.; Takamura, T. Evaluation of the Li insertion/extraction reaction rate at a vacuum-deposited silicon film anode. *Journal of Power Sources* **2005**, *146*, 445–447.
(26) Xie, J.; Imanishi, N.; Zhang, T.; Hirano, A.; Takeda, Y.; Yamamoto, O. Li-ion diffusion in amorphous Si films prepared by RF magnetron sputtering: A comparison of using liquid and polymer electrolytes. *Materials Chemistry and Physics* **2010**, *120*, 421–425.
(27) Ding, N.; Xu, J.; Yao, Y. X.; Wegner, G.; Fang, X.; CHen, C. H.; Lieberwirth, I. Determination of the diffusion coefficient of lithium ions in nano-Si. *Solid State Ionics* **2009**, *180*, 222–225.
(28) Li, J.; Xiao, X.; Yang, F.; Verbrugge, M. W.; Cheng, Y.-T. Potentiostatic Intermittent Titration Technique for Electrodes Governed by Diffusion and Interfacial Reaction. *J. Phys. Chem. C* **2011**, *116*, 1472–1478.
(29) Strauß, F.; Hüger, E.; Heitjans, P.; Trouillet, V.; Bruns, M.; Schmidt, H. Li–Si thin films for battery applications produced by ion-beam co-sputtering. *RSC Adv.* **2014**, *5*, 7192–7195.
(30) Scofield, J. H. Hartree-Slater subshell photoionization cross-sections at 1254 and 1487 eV. *Journal of Electron Spectroscopy and Related Phenomena* **1976**, *8*, 129–137.
(31) Crank, J. *The mathematics of diffusion*; Oxford university press, 1979.
(32) Pell, E. M. Diffusion Rate of Li in Si at Low Temperatures. *Phys. Rev.* **1960**, *119*, 1222.
(33) Larue, J. C. Lithium Diffusion in Silicon with Respect to Si Solar Cells. *Phys. Stat. Sol. (a)* **1971**, *6*, 143–151.
(34) Zastrow, U.; Beyer, W.; Herion, J. SIMS depth profile analysis for investigations of the lithium-diffusion in hydrogenated amorphous silicon. *Fresenius J Anal Chem* **1993**, *346*, 92–95.
(35) Sacci, R. L.; Lehmann, M. L.; Diallo, S. O.; Cheng, Y. Q.; Daemen, L. L.; Browning, J. F.; Doucet, M.; Dudney, N. J.; Veith, G. M. Lithium Transport in an Amorphous Li x Si Anode Investigated by Quasi-elastic Neutron Scattering. *J. Phys. Chem. C* **2017**, *121*, 11083–11088.
(36) Kuhn, A.; Sreeraj, P.; Pöttgen, R.; Wiemhöfer, H.-D.; Wilkening, M.; Heitjans, P. Li Ion Diffusion in the Anode Material Li 12 Si 7: Ultrafast Quasi-1D Diffusion and Two Distinct Fast 3D Jump Processes Separately Revealed by 7 Li NMR Relaxometry. *J. Am. Chem. Soc.* **2011**, *133*, 11018–11021.
(37) Wen, C. J.; Huggins, R. A. Chemical diffusion in intermediate phases in the lithium-silicon system. *Journal of Solid State Chemistry* **1981**, *37*, 271–278.

(38) Dunst, A.; Sternad, M.; Epp, V.; Wilkening, M. Fast Li + Self-Diffusion in Amorphous Li–Si Electrochemically Prepared from Semiconductor Grade, Monocrystalline Silicon: Insights from Spin-Locking Nuclear Magnetic Relaxometry. *J. Phys. Chem. C* **2015**, *119*, 12183–12192.
(39) Wang, H.; Ji, X.; Chen, C.; Xu, K.; Miao, L. Lithium diffusion in silicon and induced structure disorder: A molecular dynamics study. *AIP Advances* **2013**, *3*, 112102.
(40) Chiang, H.-H.; Lu, J.-M.; Kuo, C.-L. First-principles study of the structural and dynamic properties of the liquid and amorphous Li–Si alloys. *J. Chem. Phys.* **2016**, *144*, 34502.
(41) Fedorov, A. S.; Kuzubov, A. A.; Eliseeva, N. S.; Popov, Z. I.; Visotin, M. A.; Galkin, N. G. Theoretical Study of the Lithium Diffusion in the Crystalline and Amorphous Silicon as well as on its Surface. In *Physics and technology of nanostructured materials II*, Selected, peer reviewed papers from the Second Asia Conference on Physics and Technology of Nanostructured Materials (ASCO-Nanomat 2013), August 20-27, 2013, Vladivostok, Russia; Galkin, N., Ed.; Trans Tech Publications: Durnten-Zurich, Switzerland, 2014; pp 29–34.
(42) Brodsky, M. H.; Title, R. S. Electron Spin Resonance in Amorphous Silicon, Germanium, and Silicon Carbide. *Phys. Rev. Lett.* **1969**, *23*, 581.
(43) Pantelides, S. T. Defects in Amorphous Silicon: A New Perspective. *Phys. Rev. Lett.* **1986**, *57*, 2979–2982.
(44) Beyer, W.; Zastrow, U. Hydrogen and Lithium Diffusion in Amorphous Silicon. *MRS Proc.* **1993**, *297,* DOI: 10.1557/PROC-297-285.
(45) Beyer, W. Diffusion and evolution of hydrogen in hydrogenated amorphous and microcrystalline silicon. *Solar Energy Materials and Solar Cells* **2003**, *78*, 235–267.
(46) Luo, Y.-R. *Comprehensive handbook of chemical bond energies*. New version of: Handbook of bond dissociation energies in organic compounds; CRC Press: Boca Raton, 2007.
(47) Jackson, W. B.; Tsai, C. C. Hydrogen transport in amorphous silicon. *Phys. Rev. B* **1992**, *45*, 6564.
(48) Tritsaris, G. A.; Zhao, K.; Okeke, O. U.; Kaxiras, E. Diffusion of Lithium in Bulk Amorphous Silicon: A Theoretical Study. *J. Phys. Chem. C* **2012**, *116*, 22212–22216.
(49) Pearton, S. J.; Corbett, J. W.; Stavola, M. *Hydrogen in Crystalline Semiconductors*; Springer Series in Materials Science 16; Springer Berlin Heidelberg: Berlin, Heidelberg, 1992.
(50) Kissinger, G.; Pizzini, S. *Silicon, germanium, and their alloys: Growth, defects, impurities, and nanocrystals*; CRC Press, Taylor & Francis Group: Boca Raton, FL, 2015.
(51) Street, R. A. Trapping parameters of dangling bonds in hydrogenated amorphous silicon. *Appl. Phys. Lett.* **1982**, *41*, 1060–1062.

TOC-Graphic: